



LAWRENCE  
LIVERMORE  
NATIONAL  
LABORATORY

# Enhanced Infrared Surveillance Imaging Report for NA-22

C. J. Carrano

October 17, 2005

## **Disclaimer**

---

This document was prepared as an account of work sponsored by an agency of the United States Government. Neither the United States Government nor the University of California nor any of their employees, makes any warranty, express or implied, or assumes any legal liability or responsibility for the accuracy, completeness, or usefulness of any information, apparatus, product, or process disclosed, or represents that its use would not infringe privately owned rights. Reference herein to any specific commercial product, process, or service by trade name, trademark, manufacturer, or otherwise, does not necessarily constitute or imply its endorsement, recommendation, or favoring by the United States Government or the University of California. The views and opinions of authors expressed herein do not necessarily state or reflect those of the United States Government or the University of California, and shall not be used for advertising or product endorsement purposes.

This work was performed under the auspices of the U.S. Department of Energy by University of California, Lawrence Livermore National Laboratory under Contract W-7405-Eng-48.

**Enhanced Infra-red Surveillance Imaging Report**  
**For NA-22**  
**By C. J. Carrano, LLNL**  
**Sept. 2005**

**Abstract**

The purpose of this report is to describe our work on enhanced infra-red (IR) surveillance using speckle imaging for NA-22. Speckle imaging in this context is an image post-processing algorithm that aims to solve the atmospheric blurring problem of imaging through horizontal or slant path turbulence. We will describe the IR imaging systems used in our data collections and show imagery before and after speckle processing. We will also compare IR imagery with visible wavelength imagery of the same target in the same conditions and demonstrate how going to longer wavelengths can be beneficial in the presence of strong turbulence.

**1.0 Introduction**

Most of our enhanced surveillance with speckle imaging work has been performed at visible wavelengths<sup>1,2,3</sup>. We now investigate and report on speckle imaging at longer wavelengths. Infra-red imaging provides a number of benefits compared to visible imaging and consequently is a mainstay of many US government tactical surveillance and targeting systems. We already know that IR imaging can be performed day or night, and even see through obscurants, but in terms of speckle imaging, going to the IR will extend the range and/or turbulence strengths over which high-resolution imagery may be obtained compared to visible wavelengths. This is because atmospheric turbulence has a smaller effect on images at longer wavelengths, therefore, more turbulence and/or longer ranges can be accommodated.

**2.0 Near infra-red (NIR) imaging**

2.1 System description

The imaging system consisted of several key components which are listed below:

- Celestron, 8-inch, f/10, Schmidt-Cassegrain telescope
- 3x Barlow lens to increase magnification to 5 urad/pixel
- Indigo Phoenix NIR camera (320x256 pixels, 0.9-1.7  $\mu$ m spectral band, 30  $\mu$ m pixel pitch)
- Data acquisition computer

A photograph of the setup is shown in Figure 1. We transported the system to a location onsite at LLNL that had a clear view of the Livermore dump and surrounding hillsides which are approximately 7-8 km distant. We expected to find vehicles and other interesting objects to image, which was certainly the case. Figure 2 shows a wide-field photograph of our imaging target region from our data collection site.



Figure 1: Photograph of NIR camera attached to Celestron telescope.

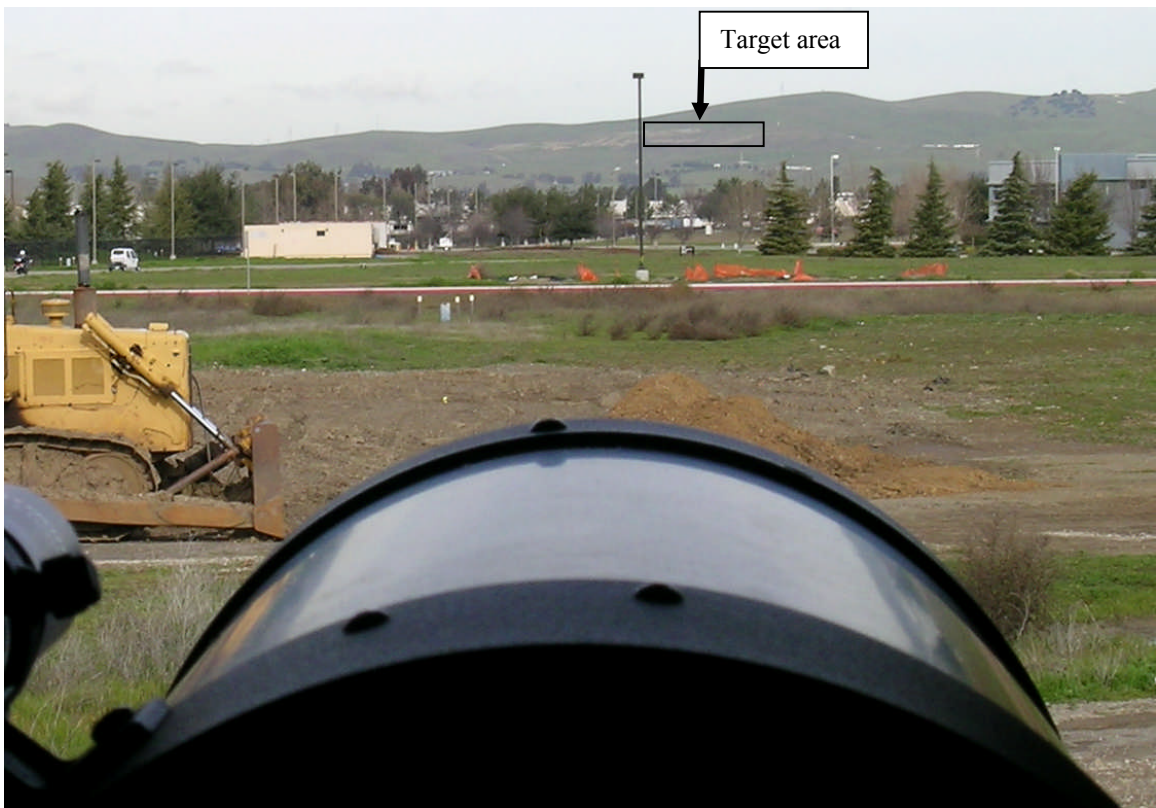


Figure 2: Photograph of target area roughly 7-8 km range from camera location at LLNL.

## 2.2 Imagery and processed results

We now show a selection of results from our NIR data collection in January-February, 2005.

### 2.2.1 Person at close range

The first result we show is that of a person imaged from roughly 0.4 kilometers away over a pure horizontal path in Figure 3. The weather was cool and calm on this winter morning. While the image quality of the sample frames does not prevent us from reading the letters or knowing there is a person standing there, the speckle processed image allows us to clearly see the facial details of the person and exhibits sharp edges on the letters. The grayscale shading in terms of object coloring can be misleading in IR wavelengths as the person was actually wearing a black hat and a black shirt and has dark hair, but nevertheless, we observe high contrast imagery.

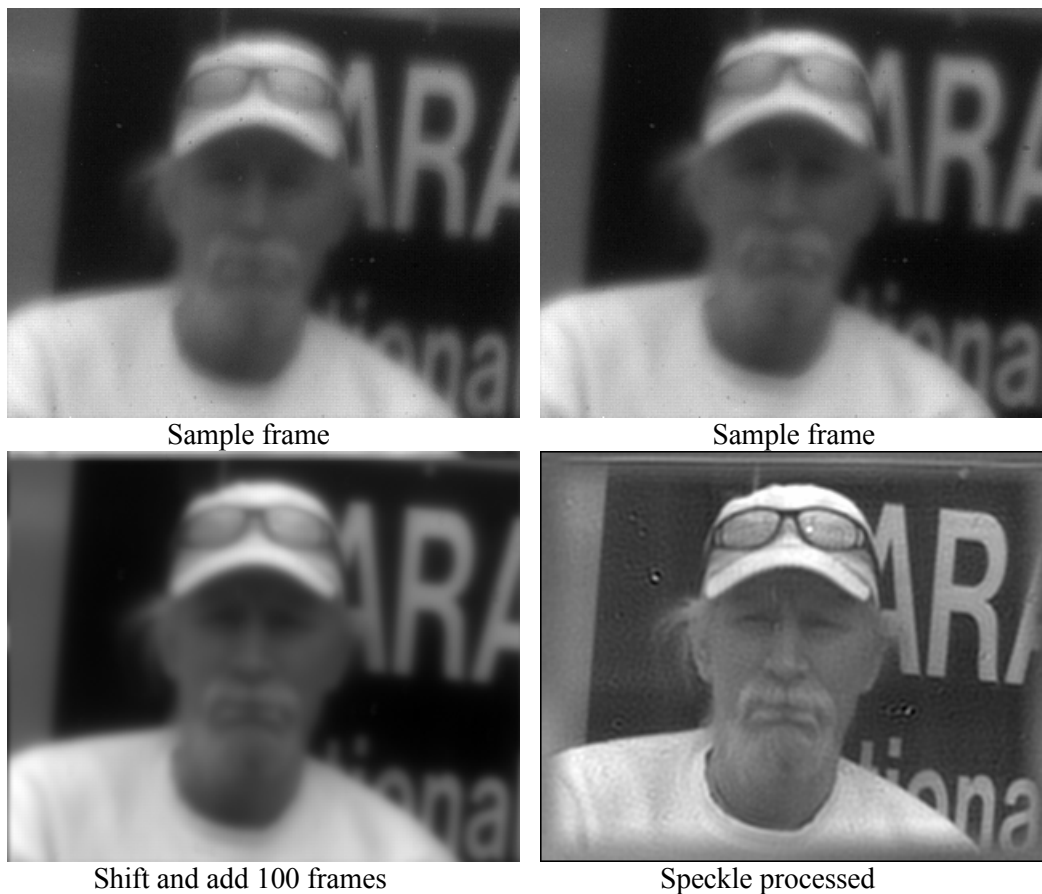


Figure 3: Face of person imaged at roughly half a kilometer range in the NIR before and after speckle processing.

### 2.2.2 Objects at 8 km range

The results we show in this section are of vehicles along with various objects such as a sign, posts, foliage, and debris at roughly 8 km range over a slightly upward looking slant path (see Figure 2). Figure 4 shows a tractor and a “ONE WAY” sign. In the speckle processed image, the sign is more clearly readable and the tractor more identifiable. In fact, when we were acquiring the imagery, we did not even know that we were looking at a vehicle until after it was speckle processed. Figure 5 shows what is probably a storage container surrounded by garbage. In the speckle processed image, everything is much higher resolution revealing greater details about the debris content. This is also evident if we look at the frequency content in a small region of the debris shown in Figure 6.

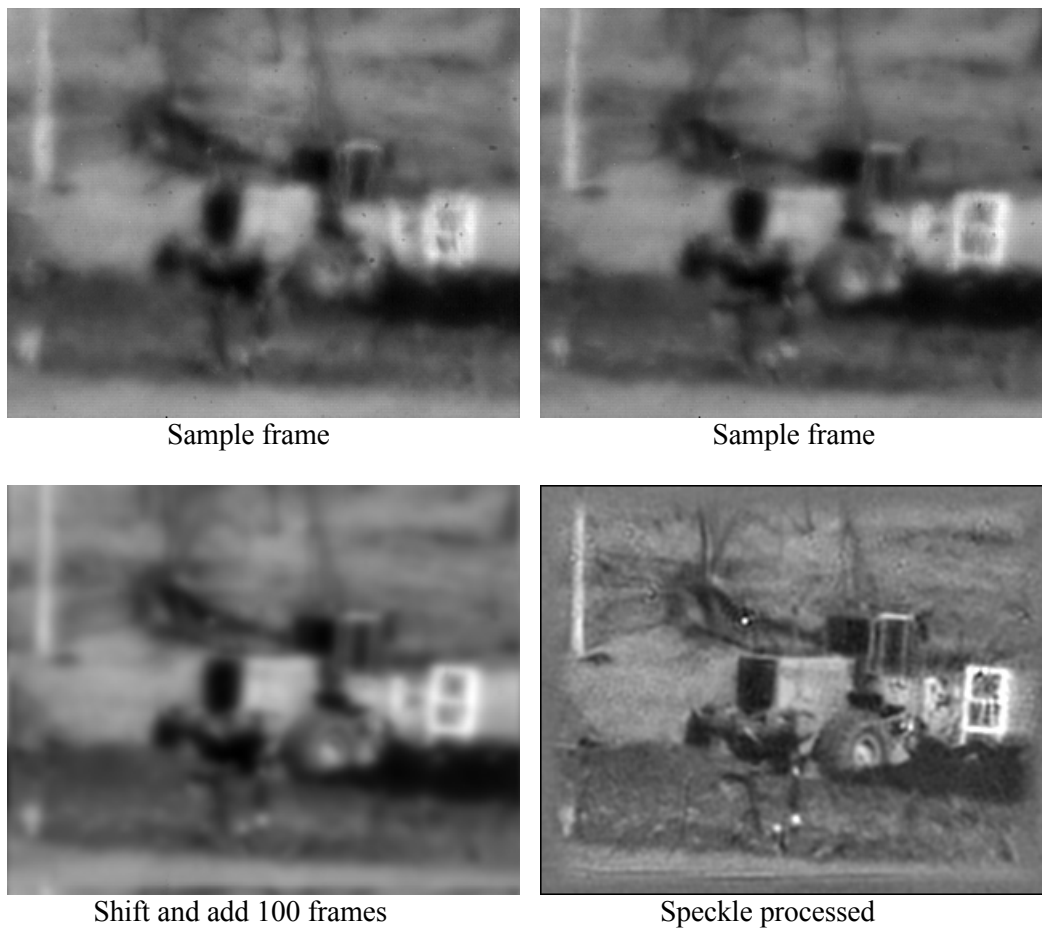


Figure 4: Tractor and sign at the Livermore dump imaged from 8 km away before and after speckle processing.

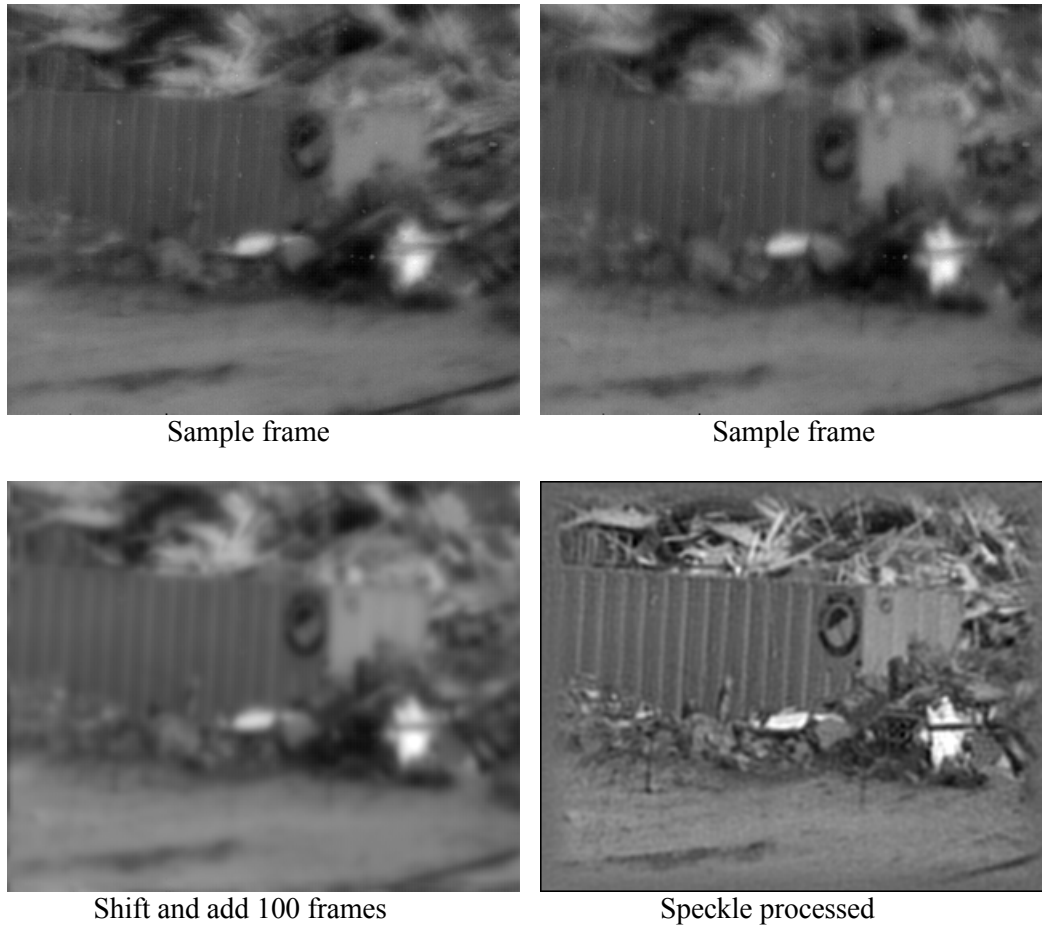


Figure 5: Storage container and garbage at the Livermore dump imaged from 8 km range before and after speckle processing.

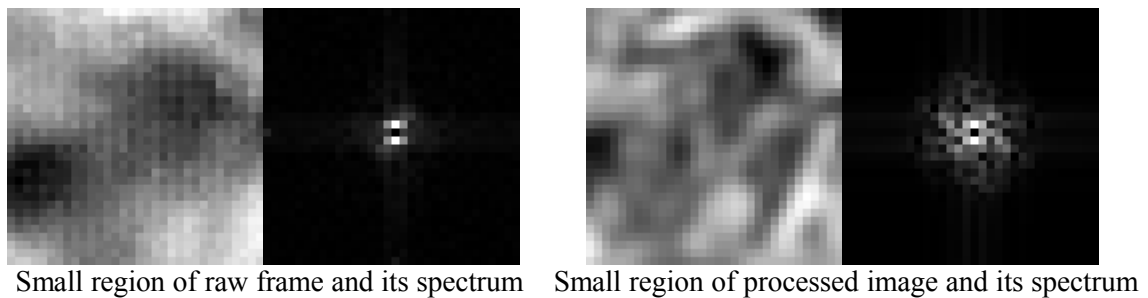


Figure 6: Magnified small regions of imagery and the magnitude of their Fourier transforms before and after speckle processing revealing lower noise and several times higher resolution.

### 3.0 Mid-wave IR (MWIR) imaging

#### 3.1 System description

The transition from NIR to MWIR was not as simple as swapping cameras. The Schmidt-Cassegrain telescope used for all the visible and NIR experiments was useless in the MWIR due

to the corrector plate being made of a material opaque to the 3-5  $\mu\text{m}$  band. As a result, employment of a new optical setup with all reflective optics was necessary. A photograph of the all reflective optic imaging setup is shown in Figure 7.

The imaging system consisted of several key components which are listed below:

- STARHOC, 8-inch, f/4, Newtonian reflector telescope
- Indigo Phoenix MWIR camera (320x256 pixels, 3.0-5.0  $\mu\text{m}$  spectral band, 30  $\mu\text{m}$  pixel pitch). Exposure time fixed at 2.3 ms. Frame rate > 100 Hz.
- Unable to use Barlow lens, so sampling is 37.5  $\mu\text{rad}/\text{pixel}$
- Data acquisition computer



Figure 7: Newtonian reflector telescope with Indigo camera attached and looking out the (open) window of our observation location.

### 3.2 Imagery and processed results

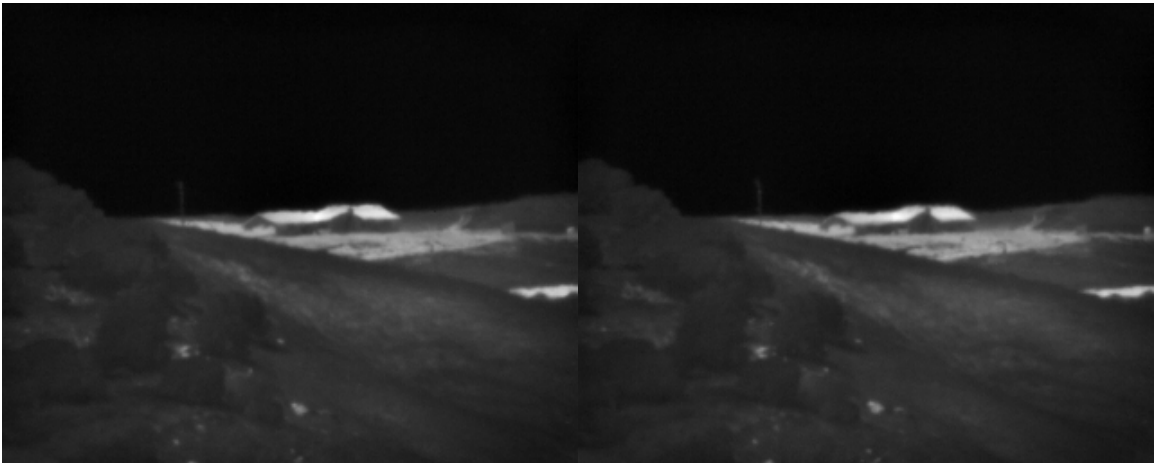
We now show a selection of results from our MWIR data collection in May, 2005. The weather during the data collection was near 90 degrees F. Arrows drawn on the picture in Figure 8 indicate the physical locations of the imagery that we will show in the next 3 subsections.



Figure 8. View from our observation location in May 2005. Arrows indicate the target locations for imagery shown in this report.

### 3.2.1 House on a hill at 9 km range

This first result we show in Figure 9 is that of a house (and surrounding foliage) on top of a hill, roughly 1100 feet above the ground level and 9 km distant from the observing site. The first thing we notice about this MWIR raw imagery is that the raw frames are not particularly that blurry. The dominant effect here is warping and waviness, which is more evident when watching a movie of the frames. The lower degree of blurriness is due to the undersampling of the aperture; we are undersampling Nyquist at 4  $\mu\text{m}$  by a factor of 3.75. The processed image doesn't have any of the waviness of the raw imagery and is much sharper than the raw imagery or the shift and add image.



Sample frame

Sample frame

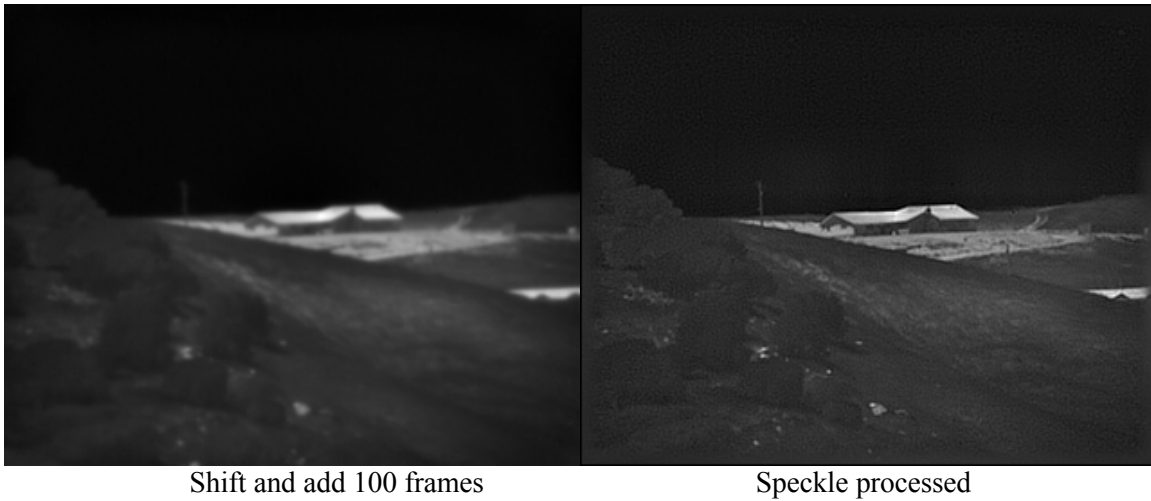
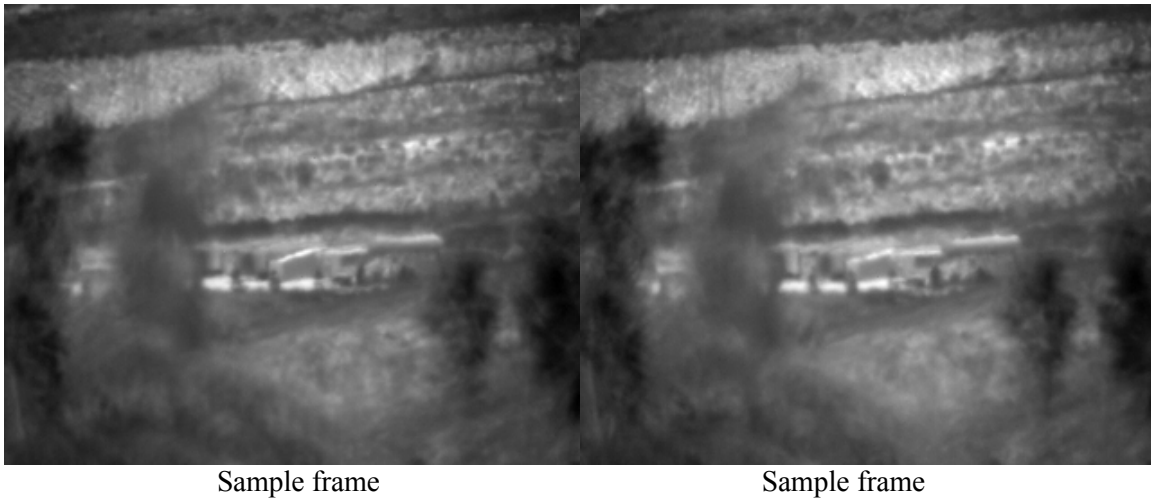


Figure 9: Image of a house on top of a hill at roughly 9 km range.

### 3.2.2 Objects at 6 km

For this next case shown in Figure 10, we pointed the telescope as close to horizontal as we could in search of stronger turbulence. As we can see, foreground trees block much of the path, limiting our ability to go purely horizontal. But by decreasing our slant angle by just over a factor of two, we noticed a significant increase in turbulence on the camera monitor during the experiment. Imagery from higher on the hill on that same day was processed with an  $r_0$  of 1.7-2.0 cm, while this dataset necessitated an  $r_0$  of 1.5 cm. (Lower  $r_0$ 's mean stronger turbulence.)



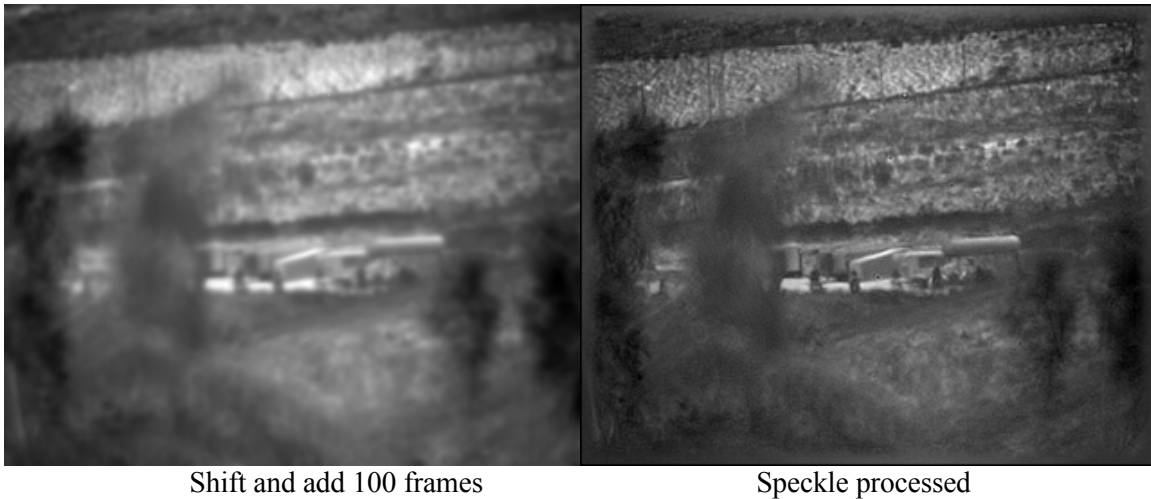
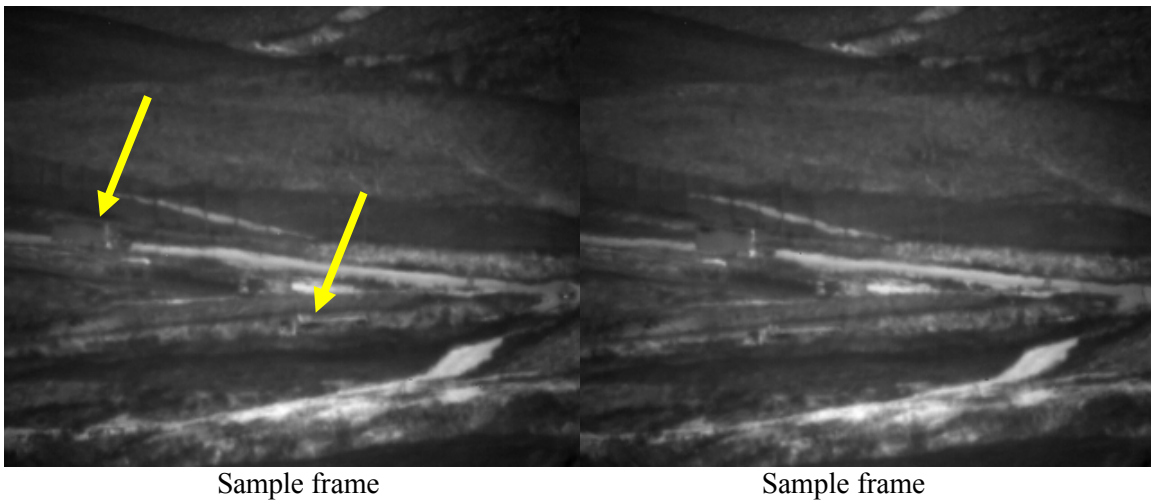


Figure 10: Objects and surrounding foliage at roughly 6 km range.

### 3.2.3 Moving trucks at 7.5 km

This last MWIR case we show is that of vehicles traveling at slow speed on a road to the dump. A sample frame from the beginning and end of the sequence are shown in Figure 11. Also shown is what happens when all 200 frames are summed together versus just the first 10 frames as well as when 200 frames are speckle processed versus just the first 10. In both 200 frame cases the vehicles are blurred out, while for the 10 frame speckle processed case, both the scene and the vehicles appear crisp and sharp.



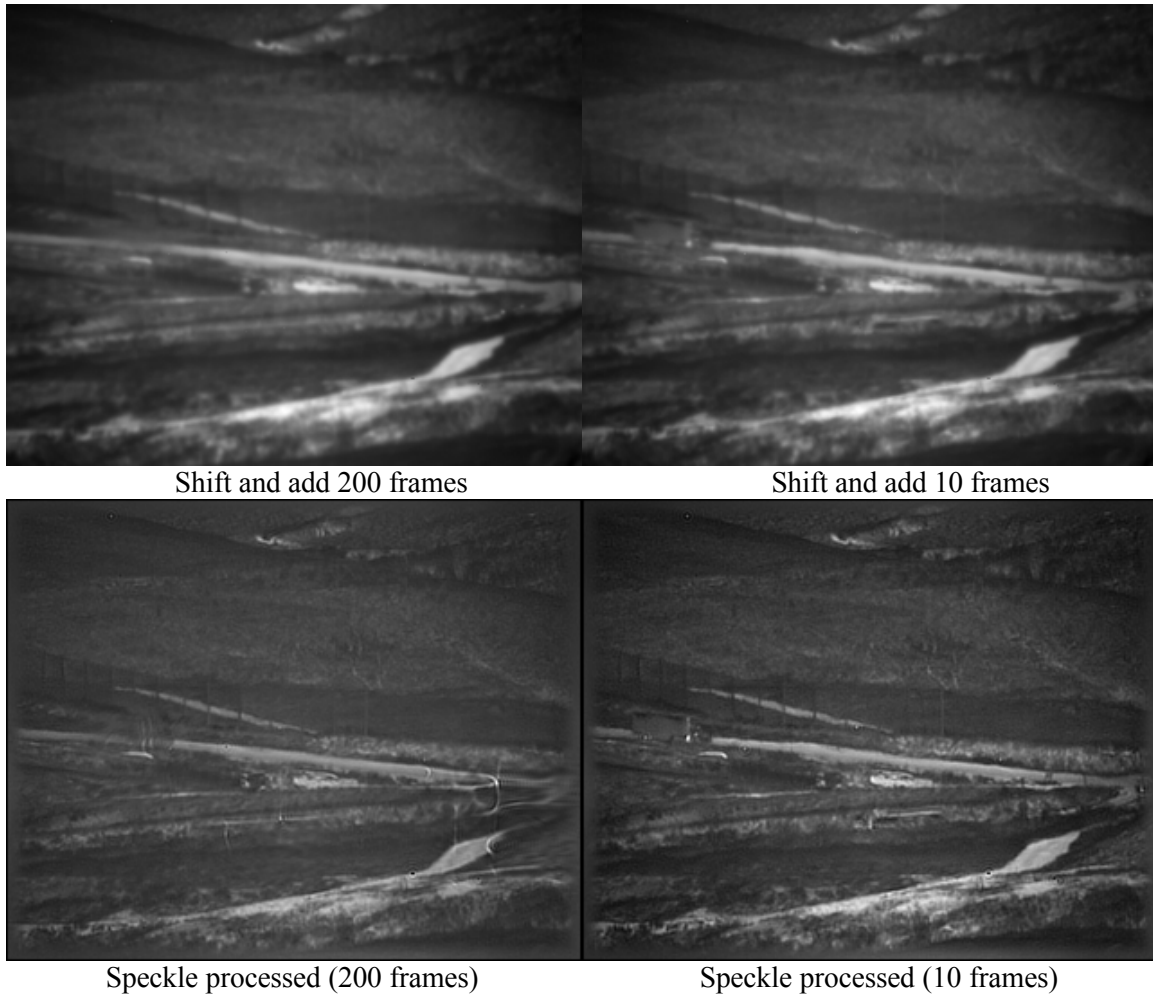


Figure 11: Vehicles traveling on a road and surrounding foliage and fence at roughly 7.5 km range.

#### 4.0 Comparison between spectral bands

##### 4.1. NIR versus Visible

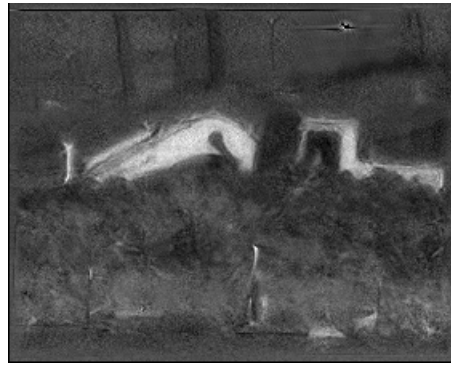
Here we show a comparison between imagery of the same target acquired at nearly the same time with the NIR camera and a visible light camera. The visible images have been rescaled to have the same sampling interval as the NIR images for easier comparison. In both cases we are using the 3x Barlow lens, giving a sampling interval in the visible of 1.12 urad/pixel and 5 urad/pixel in the NIR. Two obvious differences are noticeable in the raw shift and add images. The first is that the resolution of the visible case is slightly lower. We can see this by looking at certain small features in the visible image that are almost completely blurred out while they are still observable in the NIR image. The other difference is the contrast and appearance of the scenery owing to the varying reflectivity of different materials as a function of wavelength. For this particular scene, the NIR imagery has more pleasing contrast with better signal to noise ratio. The speckle processed results in the NIR appear to have slightly better processed resolution and with far less artifacts than in the visible. What we learn is that for this 8 km slant path, under these

atmospheric and sampling conditions, we are better off to image in the NIR if we want artifact free high-resolution images.



Shift and add 100 frames

*Visible wavelength – downsampled to NIR sample interval*



Speckle processed with  $r_0 = 0.8$  cm



Shift and add 100 frames

*NIR wavelength*



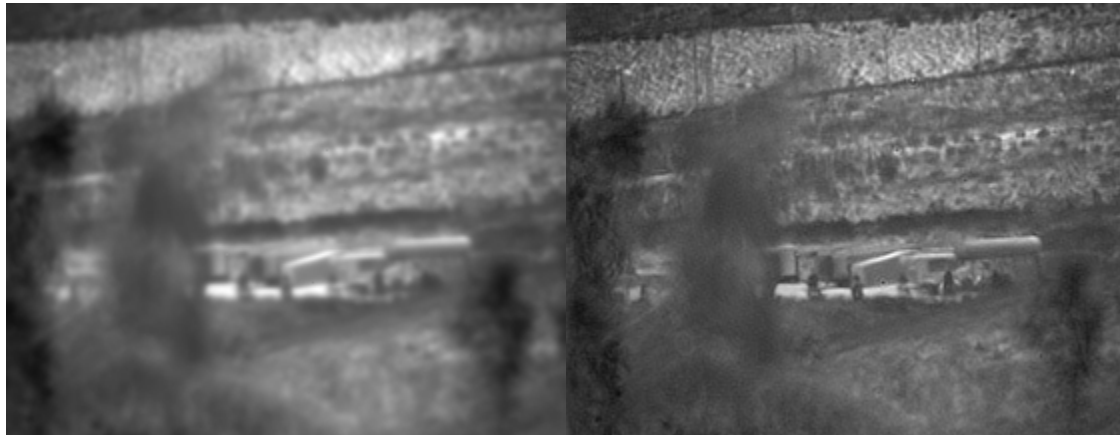
Speckle processed with  $r_0 = 1.5$  cm

Figure 12: Comparison of visible and NIR imagery of same target at 8 km range taken at nearly the same time.

#### 4.2 MWIR versus Visible

In comparing visible to MWIR, note that the diffraction limit at these two wavelengths is nearly an order of magnitude different. The diffraction limit of a 20 cm optic at 0.5  $\mu\text{m}$  is 2.5  $\mu\text{rad}$  while at 4  $\mu\text{m}$ , it is 20  $\mu\text{rad}$ . Also, the actual angular pixel sizes of each wavelength case used for the experiment are quite different as well owing to the differing physical pixel sizes. In the visible setup, we are sampling at 8.375  $\mu\text{rad}/\text{pixel}$  with no Barlow lens, while for the MWIR setup with the same telescope we are sampling at 37.5  $\mu\text{rad}/\text{pixel}$ . Figure 13 shows shift and add as well as the speckle processed results for the two wavelengths. The visible images are downsampled to the IR image size for comparison and what we see is nice reconstructions in both wavebands at those sample intervals. If we were to look at the visible imagery at full scale, such as in Figure 14, we would find that there is not much additional information available, because the atmospheric conditions are so poor here. (i.e. millimeter scale  $r_0$  in the visible) Another way to visualize this is by looking at the short exposure time averaged powerspectra at both wavelengths. On the left side of Figure 15 we see the visible powerspectrum energy falls into the noise below  $0.1(D/\lambda)$ 's or diffraction limits, while on the right side of Figure 15 we see the

MWIR powerspectrum energy is good all the way out to the edge of it's spectrum (i.e.  $4-5 (D/\lambda)$ 's). Indications from this plot are that if we had a longer focal length optic, it is possible that we could have obtained even better MWIR resolution, since we were undersampling the diffraction limit in the MWIR. Though substantial improvement in resolution is found by speckle processing the visible case, we see that the resolution advantage normally attributed the visible wavelength imaging is not the case in these conditions and the resolution is reduced to nearly that of the MWIR system. In addition, imaging in the MWIR gives nice contrast in much of the scene, such as the foliage, less observable in the visible, while other features are more observable in the visible, such as the fence posts.



Shift and add 100 frames

Speckle processed with  $r_0 = 1.5$  cm

*MWIR wavelength*



Shift and add 100 frames

Speckle processed with  $r_0 = 1.5$  mm

*Visible wavelength – downsampled to MWIR sampling interval*

Figure 13: Comparison of visible and MWIR imagery of same target at 6 km range taken at nearly the same time.

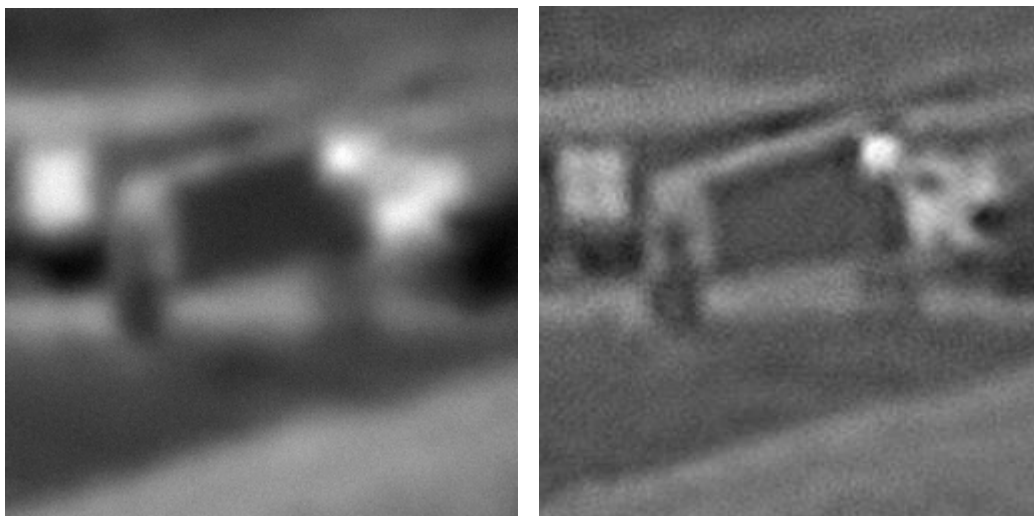


Figure 14: Small region of visible imagery at full size before and after speckle processing.

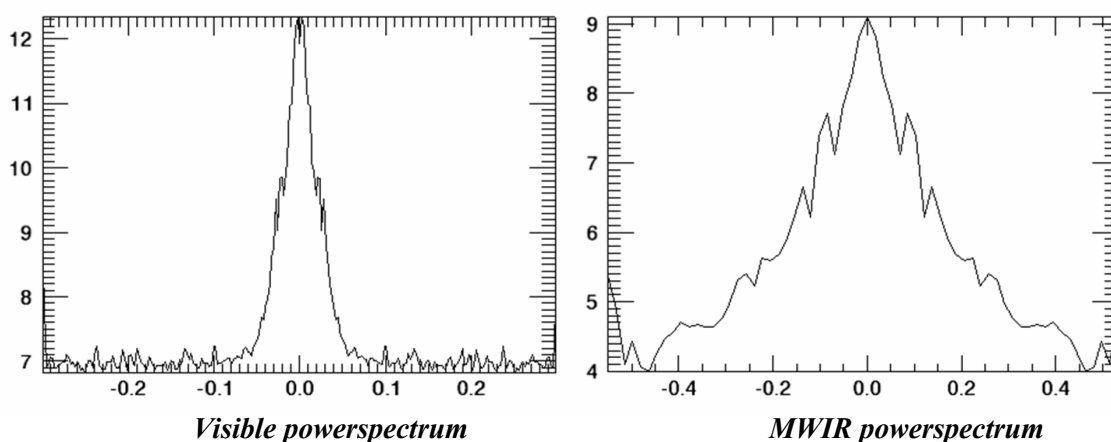


Figure 15: Comparison of 100 frame averaged powerspectrum (x-slice) of visible and MWIR section of imagery from datasets in Figure 13. The x-axis is in diffraction limit or  $D/\lambda$  units. The y-axis is on a log scale.

## 5.0 Conclusions

We have demonstrated significant resolution and contrast improvements of long range IR imagery with the use of bispectral speckle imaging. We have also demonstrated that employing longer wavelengths can be advantageous both from a signal to noise standpoint and an overall image contrast standpoint to shorter wavelengths in strong turbulence. The potential for improved long distance horizontal or slant-path imagery in any waveband from the visible through the IR through the use of speckle imaging is important for enabling an expanded range of surveillance applications, such as US government tactical surveillance and targeting systems as well as imaging systems used for standoff detection and identification of targets associated with nuclear non-proliferation.

### **Acknowledgements**

I would like to acknowledge the help of Jack Tucker and Richard Combs for their help with the IR optical system setups and data collections, and Darron Nielsen for the use of his MWIR camera.

Work performed under the auspices of the U.S. Department of Energy by the Lawrence Livermore National Laboratory under contract No. W-7405-ENG-48.

### **References**

1. C. J. Carrano, "Speckle Imaging over Horizontal Paths", Proceedings of the SPIE -High Resolution Wavefront Control: Methods, Devices, and Applications IV, 4825, 109-120, (2002)
2. C. J. Carrano, J. M. Brase, "Horizontal and Slant Path Surveillance with Speckle Imaging", AMOS Technical Conference Proceedings, (2002)
3. C. J. Carrano, "Progress in horizontal and slant-path imaging using speckle imaging", Proceedings of the SPIE-LASE2003 - Optical Engineering at the Lawrence Livermore National Laboratory, **5001** (2003) pp. 56-64